

## Parameterizing Turbulent Exchange at a Snow-Covered Surface

EDGAR L. ANDREAS,<sup>1</sup> P. OLA, G. PERSSON,<sup>2,3</sup> RACHEL E. JORDAN,<sup>4</sup>  
THOMAS W. HORST,<sup>5</sup> PETER S. GUEST,<sup>6</sup> ANDREY A. GRACHEV,<sup>2,3</sup>  
AND CHRISTOPHER W. FAIRALL<sup>2</sup>

### ABSTRACT

During the experiment to study the Surface Heat Budget of the Arctic Ocean (SHEBA), our multiple micrometeorological sites yielded over 10,000 hours of turbulent surface flux measurements during the polar winter. These measurements are relevant to the Eastern Snow Conference because polar sea ice is an ideal site for observing the fundamental processes that control turbulent exchange between the atmosphere and snow-covered surfaces. Each SHEBA site was on a horizontal surface (i.e., snow-covered sea ice) that was uniform and had no topographic variations for hundreds of kilometers in all directions. Consequently, density-driven flows that can confound measurements over land surfaces did not occur. Moreover, diurnal forcing was often weak or nonexistent; mesoscale and synoptic-scale disturbances with 1–4 day time scales were the primary mode of temporal variability. Consequently, our measurements were often in quasi-stationary conditions.

We describe our eddy-covariance measurements of the surface fluxes of momentum and sensible and latent heat and how we develop parameterizations for these fluxes. Our approach relies on Monin-Obukhov similarity theory, which, in turn, requires that we evaluate the roughness lengths for wind speed ( $z_0$ ), temperature ( $z_T$ ), and humidity ( $z_Q$ ). Here, we show only result for  $z_0$ , which we find to be independent of the friction velocity  $u_*$  in the regime (i.e., for  $u_* > 0.3$  m/s) where drifting and blowing snow has commonly been invoked to explain why  $z_0$  tended to increase with  $u_*$  in previous data sets. We attribute this increase in  $z_0$  with  $u_*$  to fictitious correlation and show that, when measured  $z_0$  is plotted against the friction velocity computed from our bulk flux algorithm, which has much less built-in correlation with  $z_0$ ,  $z_0$  is constant at about 0.23 mm in the drifting and blowing snow regime.

Keywords: bulk flux algorithm; friction velocity; Monin-Obukhov similarity; roughness length of snow; SHEBA experiment; turbulence measurements; winter sea ice

---

<sup>1</sup> NorthWest Research Associates, Inc., 25 Eagle Ridge, Lebanon, NH 03766-1900.

<sup>2</sup> NOAA Earth System Research Laboratory, Boulder, CO.

<sup>3</sup> Cooperative Institute for Research in Environ. Sciences, Univ. of Colorado, Boulder, CO.

<sup>4</sup> U.S. Army Cold Regions Research and Engineering Laboratory, Hanover, NH.

<sup>5</sup> National Center for Atmospheric Research, Boulder, CO.

<sup>6</sup> Naval Postgraduate School, Monterey, CA.

## INTRODUCTION

Snow-covered, polar sea ice is a nearly ideal surface over which to study the fundamentals of turbulent exchange between the atmosphere and a snow cover. It provides the following advantages for anyone hoping to understand the complexities of turbulent surface exchange:

- Polar sea ice in winter has the simplest geography and geometry of any surface on the planet;
- The surface is planar and at sea level;
- The surface is horizontal and, thus, does not induce density flows (e.g., katabatic winds) that are common on glaciers and over mountain snow packs;
- The surface is uniform and homogeneous for hundreds of kilometers in all directions;
- During late autumn, winter, and early spring, the polar regions experience little or no diurnal forcing, which leads to nonstationarity in atmospheric time series collected at lower latitudes.

As a consequence, turbulence parameterizations formulated from data collected over snow-covered sea ice constitute a baseline from which to develop parameterizations over more complex snow-covered surfaces: for example, mountain glaciers, patchy snow, and snow fields surrounded by higher topography or mixed vegetation.

Here we use turbulence data collected over snow-covered sea ice during SHEBA, the experiment to study the Surface Heat Budget of the Arctic Ocean, to develop a bulk turbulent flux algorithm for predicting the turbulent surface fluxes over a snow cover. The SHEBA experiment took place in and around an ice camp deployed on floating sea ice in the Beaufort Gyre (Uttal et al., 2002) and ran from October 1997 until October 1998. The data reported here come from winter conditions during SHEBA—when the sea ice was compact and snow-covered and the snow was cold and dry enough to drift and blow under wind forcing. To emphasize the simplicity of the terrain, Figure 1 shows a view of the surface that we worked over during winter.

## BULK FLUX ALGORITHM

Energy budget studies or atmospheric models with snow as the lower boundary almost always estimate the surface fluxes of momentum ( $\tau$ ) and sensible ( $H_s$ ) and latent ( $H_L$ ) heat from a bulk flux algorithm (e.g., Brun et al., 1989; Jordan et al., 1999; Bintanja, 2000; Lehning et al., 2002; Briegleb et al., 2004). In our algorithm, the relevant flux predictions take the form



Figure 1. SHEBA sea ice in late October 1997, as seen from the 10-meter level of the Atmospheric Surface Flux Group 20-meter tower. The instrument is a sonic anemometer/thermometer.

$$\tau = -\rho \overline{uw} \equiv \rho u_*^2 = \rho C_{Dr} S_r^2, \quad (1a)$$

$$H_s = \rho c_p \overline{w\theta} = \rho c_p C_{Hr} S_r (\Theta_s - \Theta_r), \quad (1b)$$

$$H_L = \rho L_v \overline{wq} = \rho L_v C_{Er} S_r (Q_s - Q_r). \quad (1c)$$

In these,  $u$ ,  $w$ ,  $\theta$ , and  $q$  are turbulent fluctuations in longitudinal wind speed, vertical wind speed, temperature, and specific humidity; the overbar indicates a time average. Also,  $\rho$  is the air density;  $c_p$ , the specific heat of air at constant pressure;  $L_v$ , the latent heat of sublimation;  $S_r$ , the average effective wind speed at reference height  $r$ ;  $\Theta_r$  and  $Q_r$ , the average potential temperature and specific humidity at  $r$ ; and  $\Theta_s$  and  $Q_s$ , the temperature and specific humidity at the snow surface. We evaluate  $Q_s$  as the saturation value at  $\Theta_s$ . Equation (1a) also defines the friction velocity,  $u_*$ .

The crux of any bulk flux algorithm is evaluating the transfer coefficients for momentum, sensible heat, and latent heat appropriate for height  $r$ —respectively,  $C_{Dr}$ ,  $C_{Hr}$ , and  $C_{Er}$  in (1). These generally derive from Monin-Obukhov similarity theory and formally are (e.g., Garratt, 1992, p. 52ff.; Andreas, 1998)

$$C_{Dr} = \frac{k^2}{[\ln(r/z_0) - \psi_m(r/L)]^2}, \quad (2a)$$

$$C_{Hr} = \frac{k^2}{[\ln(r/z_0) - \psi_m(r/L)][\ln(r/z_r) - \psi_h(r/L)]}, \quad (2b)$$

$$C_{Er} = \frac{k^2}{[\ln(r/z_0) - \psi_m(r/L)][\ln(r/z_Q) - \psi_h(r/L)]}. \quad (2c)$$

Here,  $k$  ( $= 0.40$ ) is the von Kármán constant, and  $\psi_m$  and  $\psi_h$  are empirical functions of the Obukhov length,

$$L = -\frac{\bar{T}}{kg} \left( \frac{u_*^3}{\overline{w\theta} + \frac{0.61\bar{T}}{1 + 0.61\bar{Q}} \overline{wq}} \right). \quad (3)$$

Here,  $g$  is the acceleration of gravity, and  $\bar{T}$  and  $\bar{Q}$  are surface-layer averages of the temperature and specific humidity. Because (1) and (2) are coupled through  $L$ , equations (1)–(3) must be solved iteratively.

For  $\psi_m$  and  $\psi_h$  in (2), we use Paulson's (1970) functions in unstable stratification. In stable stratification, which is the more common regime over sea ice in winter, we use the new functions reported by Grachev et al. (2007). These functions are based on our SHEBA data set and include proper treatment of a heretofore unrecognized scaling regime in very stable stratification. The  $z_0$ ,  $z_r$ , and  $z_Q$  in (2) are the roughness lengths, respectively, for wind speed, temperature, and humidity. Developing a new parameterization for  $z_0$  is the main subjects of this paper.

During SHEBA, we measured all the turbulent and mean meteorological quantities in (1) at multiple sites. In particular, we measured the momentum and sensible heat fluxes with sonic anemometer/thermometers (one is visible in Figure 1). We combined a fast-responding humidity

sensor with the sonic at one site to measure the latent heat flux. Persson et al. (2002), Grachev et al. (2005, 2007), and Andreas et al. (2006) provide further details of our SHEBA measurements.

In effect, from these measurements and as a consequence of (1), we also measured  $C_{Dr}$ ,  $C_{Hr}$ , and  $C_{Er}$  at multiple sites. For the purposes of this paper, we thus computed  $z_0$  from (2a):

$$z_0 = r \exp\left\{-\left[k C_{Dr}^{-1/2} + \psi_m(r/L)\right]\right\}. \quad (4)$$

The main SHEBA camp was our primary site. Here we had our 20-m Atmospheric Surface Flux Group (ASFG) tower, which was instrumented at five levels with identical sonic anemometer/thermometers and temperature and humidity sensors. At the 8-m level on this tower, near the sonic at that level, we had the one SHEBA-wide fast-responding humidity sensor for measuring the latent heat flux.

We also usually maintained four remote sites that were 0.4 to 10 km from the main SHEBA camp. We instrumented these sites with Flux-PAM (for portable automated mesonet) stations from the facilities pool at the National Center for Atmospheric Research (Andreas et al., 1999). These stations each had a sonic anemometer/thermometer and sensors for measuring average air temperature and humidity. We named the first four PAM sites that we deployed after the teams that were playing in the Major League Baseball League Championship Series in October 1997, while we were building the SHEBA camp: Atlanta, Baltimore, Cleveland, and Florida. Cleveland was eventually engulfed in a pressure ridge and redeployed subsequently to two new sites named Seattle and Maui. The Atlanta, Baltimore, and Florida sites, however, lasted for the entire SHEBA experiment.

#### THE ROUGHNESS LENGTH $z_0$

Figure 2 shows  $z_0$  values computed from (4) using data from our ASFG tower and plotted against friction velocity. The yellow markers are the individual hourly values to show the typical scatter in such measurements. The black circles are bin averages of these hourly data; the error bars are  $\pm 2$  standard deviations in the bin means.

Plots like Figure 2 in which measured  $z_0$  is plotted against measured  $u_*$  almost always show  $z_0$  to increase with  $u_*$  (e.g., Pomeroy and Gray, 1990; Bintanja and Van den Broeke, 1995; Brunke et

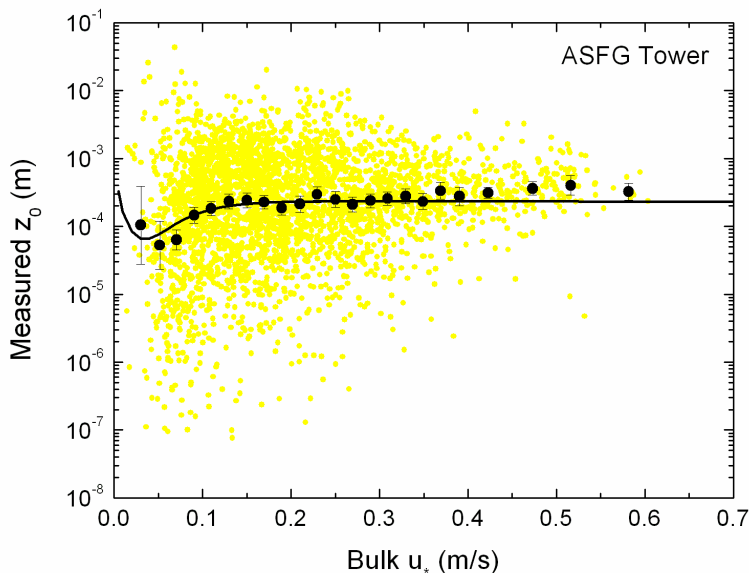


Figure 2. The roughness length  $z_0$  for 3127 hours of data (yellow circles) from our Atmospheric Surface Flux Group tower is plotted against  $u_*$  values computed from our bulk flux algorithm. The black circles are averages of these hourly data in bins that are typically 2 cm/s wide in  $u_{*,B}$ ; the error bars are  $\pm 2$  standard deviations in the bin means. The curve is (5).

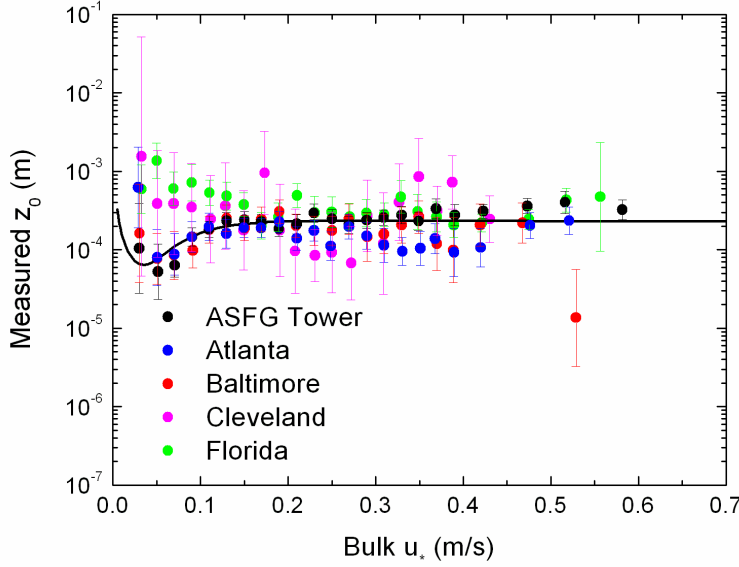


Figure 3. Bin-averaged  $z_0$  values from our Atmospheric Surface Flux Group tower (same data as in Figure 2) and from four Flux-PAM sites are plotted against friction velocities computed from our bulk flux algorithm,  $u_{*,B}$ . The error bars are  $\pm 2$  standard deviations in the bin means; the curve is (5). This plot summarizes 9159 hours of data.

al., 2006). This effect has been attributed to the influence of drifting and blowing snow (e.g., Owen, 1964; Chamberlain, 1983; Pomeroy et al., 1983; Andreas et al., 2005). But we now believe that the increase in measured  $z_0$  with measured  $u_*$  is a result of fictitious correlation: The measured  $u_*$  is embedded in  $C_{Dr}$  in (4) and thus would appear prominently on both axes in plots of measured  $z_0$  versus measured  $u_*$ .

To mitigate the effects of such fictitious correlation, we show in Figure 2 measured  $z_0$  plotted against the corresponding friction velocity computed from our bulk flux algorithm, denoted  $u_{*,B}$ . Figure 2 shows that, for such a plot,  $z_0$  does not increase with  $u_{*,B}$ . The curve in Figure 2 is thus

$$z_0 = 0.135 \frac{\nu}{u_{*,B}} + 2.30 \times 10^{-4} \tanh^3(13u_{*,B}), \quad (5)$$

where  $z_0$  is in meters when  $u_{*,B}$  is in m/s and  $\nu$ , the kinematic viscosity of air, is in  $m^2/s$ .

Figure 3 reiterates this conclusion by adding bin-averaged data from four PAM sites to the bin-averaged ASFG tower data from Figure 2. Again, (5) represents the data well; none of the four PAM sites show an increase in  $z_0$  with  $u_{*,B}$  in the region where polar snow is typically drifting and blowing: for  $u_{*,B} \geq 0.3 m/s$  (Andreas et al. 2005).

The first term on the right side of (5) models aerodynamically smooth flow and produces the dip in the curves in Figures 2 and 3 for  $0 < u_{*,B} < 0.15 m/s$ . Three of the five sites in Figure 3 follow this scaling law. The Cleveland site, which produced a scanty data set and, thus, large error bars, tends to be above this dip. The Florida site also does not follow this scaling law for reasons that we do not yet understand.

## $u_*$ COMPARISONS

To demonstrate the accuracy of (5) and our bulk flux algorithm, we show in Figure 4 comparisons of measured  $u_*$  values and values modeled with our bulk flux algorithm ( $u_{*,B}$ ) for the four SHEBA sites with the longest data records.

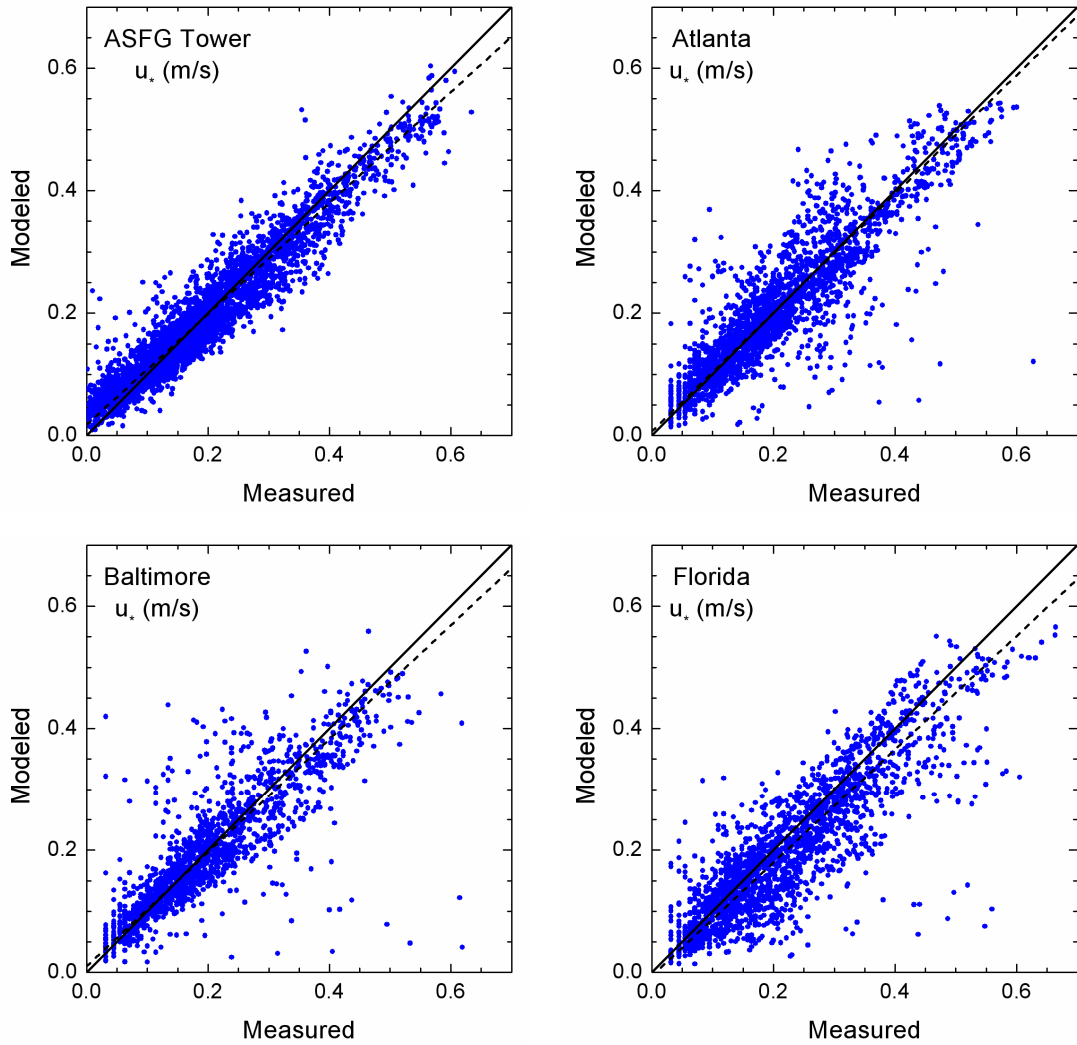


Figure 4. Comparison of  $u_*$  values measured hourly and corresponding values modeled with our bulk flux algorithm for our main ASFG tower and for three Flux-PAM sites: Atlanta, Baltimore, and Florida. In each panel, the solid line is the 1:1 relation, and the dashed line is the best fit through the data.

In each panel in Figure 4, the best fitting line through the data deviates only slightly from the 1:1 line, which shows perfect agreement. The Florida panel is the most deviant; yet even at large  $u_*$ , the trend in the data is always within about 0.03 m/s of perfect agreement. All panels in Figure 4, however, hint that the bulk flux algorithm may underestimate  $u_*$  for large  $u_*$ . This bias is small, though—typically about 0.02 m/s for the largest  $u_*$  values observed.

## SUMMARY

Our premise has been that turbulence measurements over snow-covered polar sea ice, where topography and atmospheric conditions are often quite simple in winter, can provide information on the fundamental physics that controls turbulent exchange over snow-covered surfaces in more complex terrain. From data collected during the year-long SHEBA experiment, we have thus

developed a bulk flux algorithm to predict the turbulent fluxes of momentum and sensible and latent heat from mean measured or modeled meteorological variables.

We have shown only our new parameterization for the momentum transfer, which essentially reduces to predicting the roughness length  $z_0$ . We will describe our parameterizations for the sensible and latent heat fluxes elsewhere (also see Andreas et al., 2004).

Our new algorithm for predicting  $z_0$ , (5), does not show  $z_0$  to increase with friction velocity in the regime where drifting and blowing snow typically occurs—for  $u_* \geq 0.30$  m/s—presumably because we have properly minimized the effects of fictitious correlation. Hence, according to our data, over snow-covered sea ice,  $z_0$  is essentially constant at 0.23 mm for  $0.15 \leq u_{*,B} \leq 0.65$  m/s, the upper velocity limit of our data.

We tested this new  $z_0$  algorithm in our full bulk flux algorithm and found it to do a very reliable job of reproducing our measurements of  $u_*$  (see Figure 4). We have developed FORTRAN code for this bulk flux algorithm that we would be willing to share.

## ACKNOWLEDGMENTS

The U.S. National Science Foundation (NSF) supported our initial participation in SHEBA with awards to the U.S. Army Cold Regions Research and Engineering Laboratory, NOAA's Environmental Technology Laboratory (now the Earth System Research Laboratory), the Naval Postgraduate School, and the Cooperative Institute for Research in Environmental Sciences. NSF also supported our use of the Flux-PAM stations from the facilities pool at the National Center for Atmospheric Research. Both NSF (award 06-11942) and the National Aeronautics and Space Administration (award NNX07AL77G) supported ELA at NorthWest Research Associates during the writing of this manuscript.

## REFERENCES

- Andreas EL. 1998. The atmospheric boundary layer over polar marine surfaces. *Physics of Ice-Covered Seas*, Vol. 2, M. Leppäranta (Ed.), Helsinki University Press: 715–773.
- Andreas EL, Fairall CW, Guest PS, Persson POG. 1999. An overview of the SHEBA atmospheric surface flux program. Preprints, Fifth Conference on Polar Meteorology and Oceanography, 10–15 January 1999, Dallas, TX, American Meteorological Society: 411–416.
- Andreas EL, Jordan RE, Guest PS, Persson POG, Grachev AA, Fairall CW. 2004. Roughness lengths over snow. Preprints, 18th Conference on Hydrology, 12–16 January 2004, Seattle, WA, American Meteorological Society: CD-ROM JP4.31, 8 pp.
- Andreas EL, Jordan RE, Makshtas AP. 2005. Parameterizing turbulent exchange over sea ice: The Ice Station Weddell results. *Boundary-Layer Meteorology* **114**: 439–460.
- Andreas EL, Claffey KJ, Jordan RE, Fairall CW, Guest PS, Persson POG, Grachev AA. 2006. Evaluations of the von Kármán constant in the atmospheric surface layer. *Journal of Fluid Mechanics* **559**: 117–149.
- Bintanja R. 2000. Surface heat budget of Antarctic snow and blue ice: Interpretation of spatial and temporal variability. *Journal of Geophysical Research* **105** (D19): 24,387–24,407.
- Bintanja R, Van den Broeke MR. 1995. Momentum and scalar transfer coefficients over aerodynamically smooth Antarctic surfaces. *Boundary-Layer Meteorology* **74**: 89–111.
- Briegleb BP, Bitz CM, Hunke EC, Lipscomb WH, Holland MM, Schramm JL, Moritz RE. 2004. Scientific description of the sea ice component in the Community Climate System Model, version three. NCAR Technical Note NCAR/TN-463+STR, National Center for Atmospheric Research, Boulder, CO: 70 pp.
- Brun E, Martin E, Simon V, Gendre C, Coleou C. 1989. An energy and mass model of snow cover suitable for operational avalanche forecasting. *Journal of Glaciology* **35**: 333–342.
- Brunke MA, Zhou M, Zeng X, Andreas EL. 2006. An intercomparison of bulk aerodynamic algorithms used over sea ice with data from the Surface Heat Budget of the Arctic Ocean (SHEBA) experiment. *Journal of Geophysical Research* **111** (C09001): DOI 10.1029/2005JC002907, 20 pp.

- Chamberlain AC. 1983. Roughness length of sea, sand, and snow. *Boundary-Layer Meteorology* **25**: 405–409.
- Garratt JR. 1992. *The Atmospheric Boundary Layer*. Cambridge University Press: 316 pp.
- Grachev AA, Fairall CW, Persson POG, Andreas EL, Guest PS. 2005. Stable boundary-layer scaling regimes: The SHEBA data. *Boundary-Layer Meteorology* **116**: 201–235.
- Grachev AA, Andreas EL, Fairall CW, Guest PS, Persson POG. 2007. SHEBA flux-profile relationships in the stable atmospheric boundary layer. *Boundary-Layer Meteorology* **124**: 315–333.
- Jordan RE, Andreas EL, Makshtas AP. 1999. Heat budget of snow-covered sea ice at North Pole 4. *Journal of Geophysical Research* **104** (C4): 7785–7806.
- Lehning M, Bartelt P, Brown B, Fierz C. 2002. A physical SNOWPACK model for the Swiss avalanche warning. Part III: Meteorological forcing, thin layer formation and evaluation. *Cold Regions Science and Technology* **35**: 169–184.
- Owen PR. 1964. Saltation of uniform grains in air. *Journal of Fluid Mechanics* **20**: 225–242.
- Paulson CA. 1970. The mathematical representation of wind speed and temperature profiles in the unstable atmospheric surface layer. *Journal of Applied Meteorology* **9**: 857–861.
- Persson POG, Fairall CW, Andreas EL, Guest PS, Perovich DK. 2002. Measurements near the Atmospheric Surface Flux Group tower at SHEBA: Near-surface conditions and surface energy budget. *Journal of Geophysical Research* **107** (C10): DOI 10.1029/2000JC000705, 35 pp.
- Pomeroy JW, Gray DM. 1990. Saltation of snow. *Water Resources Research* **26**: 1583–1594.
- Pomeroy JW, Gray DM, Landine PG. 1993. The Prairie Blowing Snow Model: Characteristics, validation, operation. *Journal of Hydrology* **144**: 165–192.
- Uttal T, and 27 others. 2002. Surface Heat Budget of the Arctic Ocean. *Bulletin of the American Meteorological Society* **83**: 255–275.